



HAL
open science

FLAPPING INSTABILITY OF AN ATOMIZED LIQUID JET

Jean-Philippe Matas, Alain H. Cartellier

► **To cite this version:**

Jean-Philippe Matas, Alain H. Cartellier. FLAPPING INSTABILITY OF AN ATOMIZED LIQUID JET. Proceedings of ASME 2010 3rd Joint US-European Fluids Engineering Summer Meeting and 8th International Conference on Nanochannels, Microchannels, and Minichannels, Aug 2010, Montreal, Canada. pp.FEDSM - ICNMM2010-31259. <hal-00704304>

HAL Id: hal-00704304

<https://hal.science/hal-00704304v1>

Submitted on 5 Jun 2012

HAL is a multi-disciplinary open access archive for the deposit and dissemination of scientific research documents, whether they are published or not. The documents may come from teaching and research institutions in France or abroad, or from public or private research centers.

L'archive ouverte pluridisciplinaire **HAL**, est destinée au dépôt et à la diffusion de documents scientifiques de niveau recherche, publiés ou non, émanant des établissements d'enseignement et de recherche français ou étrangers, des laboratoires publics ou privés.



HAL Authorization

FEDSM – ICNMM2010-31259

FLAPPING INSTABILITY OF AN ATOMIZED LIQUID JET

Jean-Philippe Matas
LEGI – CNRS
Université de Grenoble
BP 53

38041 Grenoble Cedex 9, France

Alain Cartellier
LEGI – CNRS
Université de Grenoble
BP 53

38041 Grenoble Cedex 9, France

ABSTRACT

We present an experimental study of the flapping instability which appears when a coaxial liquid jet is atomized by a cocurrent fast gas stream. When primary atomization does not lead to a total break-up of the liquid jet, it undergoes a large-wavelength instability, characterized by very large amplitude oscillations, and can break into large liquid fragments whose typical size is the jet diameter. These large liquid fragments, and consequently the flapping instability, are to be avoided in applications related to combustion where liquid droplets need to be as small as possible. We carried out experiments with air and water coaxial jets, with a gas/liquid velocity ratio of order 50. We studied the consequence of the flapping instability on the break-up of the liquid jet. Measurements of the frequency of the instability were carried out. We suggest a mechanism where the flapping instability could be triggered by non axisymmetrical KH modes.

INTRODUCTION

Airblast, or assisted atomization of a liquid jet is fundamental to a large number of applications. In this process the liquid is stripped from a cylindrical jet by a fast co-current air-stream, and a spray is produced¹. Applications range from injectors in turboreactors, to cryotechnic rocket engines with LOX/H₂. This process is widely used, and has proven reliable, but the mechanism by which the liquid bulk is broken into droplets is still subject to controversy. A better understanding of the different stages of the atomization process could help improve the efficiency of combustion, and decrease the amount of emissions.

Experiments carried out by coworkers on a plane mixing layer^{2,3} and on a coaxial injector⁴ have shown that the liquid break up is the result of two successive instabilities⁵. The first instability is analogous to a Kelvin-Helmholtz instability, and leads to the formation of waves at the interface between the liquid and the fast gas stream. However, while Kelvin-Helmholtz instability involves a discontinuity of the velocity profile between the gas and liquid phases, the instability involved here has been shown to rely on the smoothness of the velocity profile, namely on the finite thickness of the gas vorticity layer. Within an inviscid approximation, it predicts that the wavelength λ of the surging waves will be given by^{2,5}:

$$\lambda_{KH} = C_{KH} (\rho_L/\rho_G)^{1/2} \delta_G \quad (1)$$

with δ_G thickness of the gas boundary layer, ρ_L and ρ_G the liquid and gas densities and $C_{KH} \approx 4$ a dimensionless coefficient. The axisymmetric waves resulting from this instability are next accelerated by the fast gas stream, and undergo a Rayleigh-Taylor transverse instability, leading to the formation of liquid ligaments^{5,6,7}. These ligaments grow and will eventually break into droplets, whose size is therefore controlled by the thickness of ligaments, i.e. the wavelength of the R-T instability.

If the liquid intact length is larger than the potential cone, as is the case in our experiment, atomization of the liquid jet is incomplete: while small droplets are still produced in the potential cone region, far downstream the liquid jet ends up breaking into large liquid lumps. Just before its break-up, the liquid jet downstream the potential cone exhibits a striking “oscillating” aspect, in which the jet undergoes oscillations of a

wavelength large compared to the jet diameter (see figure 1). Our study is devoted to this large scale instability, which we dub the “flapping” instability.

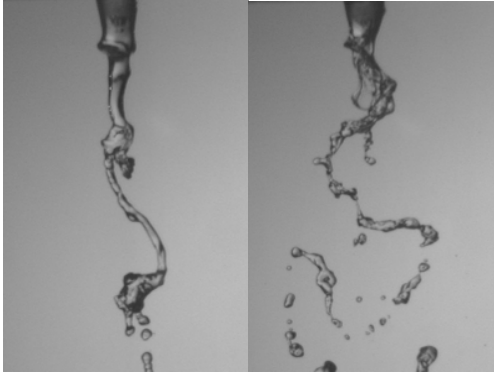


Figure 1: Instability of a liquid jet in airblast atomization for: a) $U_G = 25 \text{ m/s}$ and $U_L = 0.15 \text{ m/s}$; b) $U_G = 30 \text{ m/s}$ and $U_L = 0.15 \text{ m/s}$.

The configuration used in our experiment is quite simple: a round vertical liquid jet is entrained by a fast coaxial annular gas stream (figure 2). Injection is made through smooth convergent nozzles. The contraction is of a factor 6.9 for the liquid jet (exit diameter 8 mm), and 6 for the gas jet (outer exit diameter 11.4 mm). The convergence in the injector ensures that the intensity of perturbations is reduced. The liquid is water. Gas flow is measured with a mass flowmeter (Brooks Instruments), and liquid flow is measured with a rotameter (Kobold).

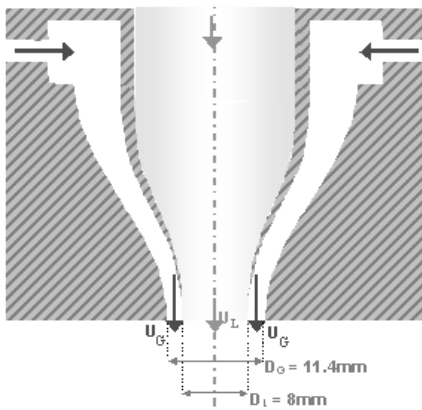


Figure 2: Sketch of the injector.

The liquid velocity U_L was varied in the range $[0.11 \text{ m/s}, 1 \text{ m/s}]$, and the gas velocity U_G in the range $[15 \text{ m/s}, 60 \text{ m/s}]$. For these ranges of velocities and the smooth convergent injector

we used, the flow is laminar in the liquid and gas boundary layers. The three dimensional structure of the flow was captured with a single camera and a vertical mirror placed at an angle of 45° next to the nozzle (see figure 3) : this device allows to capture on a same frame the front view and side view of the atomized jet, and consequently the three dimensional geometry of the flow. The camera is a high speed camera (Phantom v12), and frames are taken at a frequency in the range $[500 \text{ im/s}; 2000 \text{ im/s}]$ depending on the gas velocity and the expected frequency of the instability.

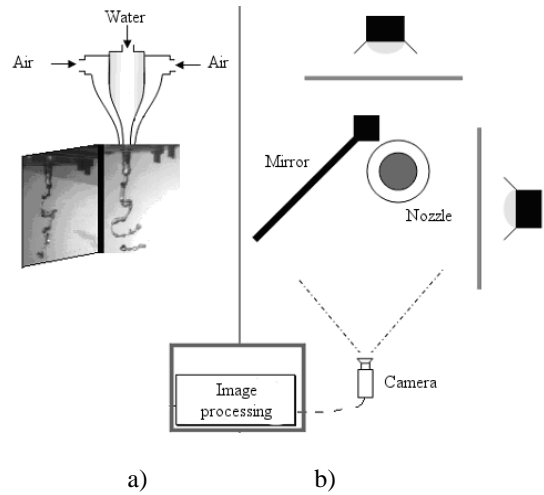


Figure 3: Sketch of the experimental set-up a) Front view ; b) Top view

Figure 4a shows the aspect of the liquid jet for gas and liquid velocities of $U_G = 40 \text{ m/s}$ and $U_L = 0.3 \text{ m/s}$ respectively. For this regime, a large number of small drops are produced near the injection, when liquid is stripped from the bulk of the jet by the fast air stream. However, it can be seen on figure 4 that large liquid fragments remain intact on the axis of the jet: though the jet undergoes a strong destabilization, these fragments cause the formation of large drops far downstream. This destabilization of the bulk of the jet is due to the flapping instability studied in this work. When the gas velocity is decreased, the growth-rate of the K-H and R-T instabilities is strongly reduced and the flapping instability becomes the dominant mechanism in the break-up of the jet: liquid is not stripped from the jet anymore (see figure 1). This instability of relatively large wavelength leads the jet to twist and break into fragments whose size is of order R .

The flapping instability is therefore especially relevant in situations when K-H and R-T instabilities fail to completely atomize the jet: this occurs in particular when the length of the gas potential cone (shown in dotted line on the sketch of figure 4b) is shorter than the liquid intact length. In our experiment this is generally true. This means that the ultimate break-up of the jet is likely to be controlled by the flapping instability.

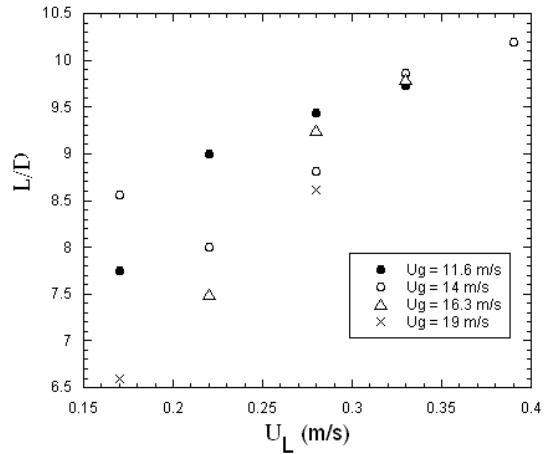
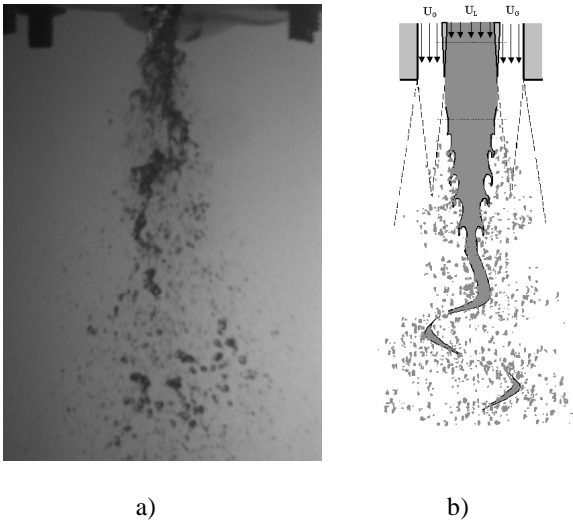


Figure 5: Liquid intact length L of the jet nondimensionalized by the liquid injector diameter D , as a function of liquid and gas velocity.

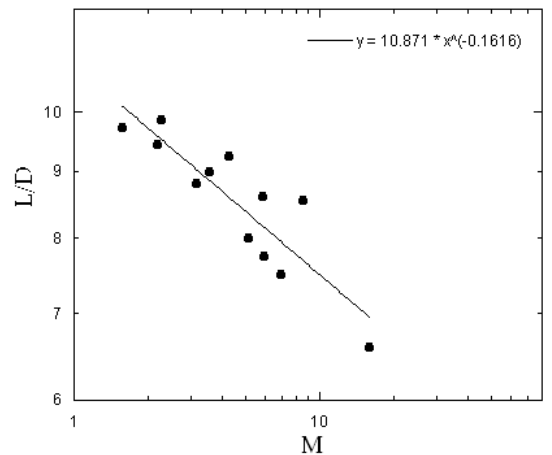


Figure 6: Logarithmic plot of the ratio L/D as a function of M . The equation of the power law fit shows a much slower decrease than the predicted $M^{-1/2}$ scaling ².

Figure 4 : a) Airblast atomization for $U_G = 40$ m/s and $U_L = 0.3$ m/s ; b) sketch emphasizing how the flapping instability creates large liquid fragments.

In order to measure the intact length of the liquid jet, the images taken with the device shown on figure 3 are processed allowing to the following sequence: the images are thresholded, we use a Matlab routine to find all paths on the image, and the jet is taken to be the longer path on each image. The intact length is taken to be the distance between the injector and the point belonging to the jet which is farthest from the injector. The intact length for a given set of gas and liquid velocity is averaged over 300 images. This process is only carried out for the front images of the jet (the mirror images are not used for this measurement). The intact length L is then nondimensionalized by the liquid jet diameter D , results are shown on figure 5.

The data of figure 5 show that as expected the liquid intact length decreases with increasing gas velocity U_g , and increases with increasing liquid velocity U_l . These measurements were only carried out for conditions where the flapping instability was present, i.e. the liquid jet exhibits large scale oscillations. Raynal (1997) ² proposed a scaling for the liquid intact length: $L/D \approx 6/\sqrt{M}$ where M is the momentum flux ratio $M = \rho_G U_G^2 / \rho_L U_L^2$. This scaling was verified experimentally in his plane shear layer experiment (liquid sheet flowing on a solid wall and atomized by a single gas stream).

In figure 6 we plot the ratio L/D as a function of M : it can be seen that though M appears to be a relevant parameter (the data of figure 5 are collapsed), the scaling law observed experimentally is quite different from the one predicted ². The decrease of L/D with M is much slower, and the values of L/D are significantly larger (longer relative intact length). This could be due to the fact that for our conditions the liquid intact length is set not only by the amount of fluid stripped by the gas from the jet, but also by the amplitude of the flapping instability. As mentioned above, this is mainly because the liquid intact length largely exceeds the length of the potential cone.

We next show measurements of the angle of aperture of the jet: these measurements are taken by superposing all images obtained for a given set of conditions. Figure 7 shows an example of result for this operation, for a liquid velocity $U_L =$

0.28 m/s and a gas velocity $U_g = 14$ m/s. The resulting image shows that there is a constant angle over a relatively large distance. The angle is measured in the region close to the injector, where the edges of the superposition are cleaner. We plot the measured angle when gas and liquid velocities are varied on figure 8. As expected, the angle increases with the gas velocity and decreases with increasing liquid velocity, i.e. when the momentum of the liquid is increased. The measurements for the lowest liquid velocity (UI = 0.17 m/s, represented by crosses on figure 8) stray a bit from this trend: this could be due to the fact that for this very low liquid velocity the jet is extremely thin a couple of diameters downstream the injector (due to its acceleration), and therefore easily deviated by the gas stream.



Figure 7 : Superposition of the successive positions of the jet, for $U_g = 14$ m/s and $UI = 0.28$ m/s.

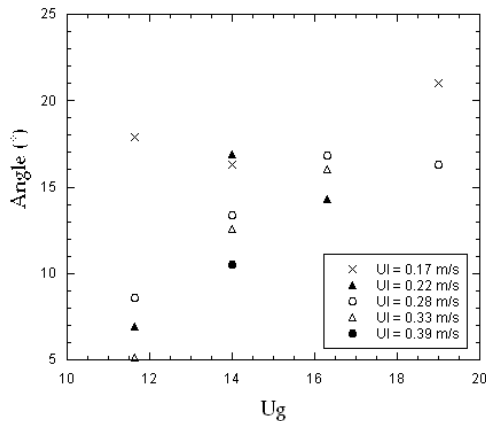


Figure 8: Angle of aperture of the jet as a function of gas velocity, for different liquid velocities.

Measurement of the wavelength of the instability has been attempted, but results are inconclusive due to the strong spatial variation of the wavelength as a function of the downstream distance: this is evidenced on figure 1b for example, where it can be seen that the first wavelength is significantly smaller than the second one (presumably due to the increase in velocity of the liquid). We therefore choose to focus instead on the

frequency of the instability.

The main difficulty for this measurement is that the flapping instability occurs roughly within a same plane, but a plane of changing orientation. The orientation of the plane of oscillation changes after a few periods, and appears to be random. In order to get rid of the tridimensionality of the instability, the images taken with the device shown in figure 3 are processed according to the following procedure: images are thresholded – only the dark region connected to the injector is retained (drops and detached ligaments are removed) – the center of this region for a given line is computed on the mirror image (this is position x) and on the front image (position y) – the distance of the jet center from the axis of the injector is then defined as $r = (x^2 + y^2)^{1/2}$ – the variations of r as a function of time are calculated for several heights (distances from the injector) – a Fourier transform of this signal yields the frequency of the oscillation.

We find that the maximum frequency is independent of the distance from the injector, provided that the measurement is made far enough from the injector. Measurements close to the injector might be affected by the Kelvin-Helmholtz instability: the latter instability is expected to produce axisymmetric waves close to the injector, but any alteration to the symmetry of the waves could induce a variation of the distance r (distance of the jet center from the axis) at the KH frequency. This is why we take care to measure the frequency of the flapping instability farther downstream, in regions where the flapping is visually predominant (criterion: the axis of the jet is displaced from the axis of the injector of a distance larger than R).

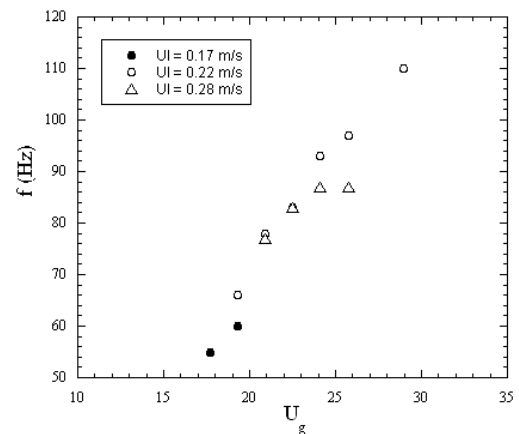


Figure 9: Frequency of the flapping instability as a function of gas velocity, for different liquid velocities.

The frequency of the flapping instability, shown on figure 9, increases with gas velocity. Only the points where a maximum frequency was clearly apparent in the spectrum were kept for the results of figure 9. We can compare these data points with the measurements of the Kelvin-Helmholtz instability carried out in a

previous experiment (see figure 10). The KH instability was measured just below the injector, by aiming a laser at the edge of the jet, and analyzing the signal received by a photodiode located opposite the laser: the signal is periodically interrupted by the KH waves, and the frequency can be measured precisely up to much larger velocities than with image processing methods. It can be seen on figure 10 that the frequency of the KH instability is slightly larger than the flapping instability, but that both frequencies are relatively close. We emphasize that both instabilities were measured at different locations: very close to the injector for the KH instability, and far downstream for the flapping: measurements of both series were made as independent as possible, and the closeness of the results is probably a clue to the physical link between both instabilities in our experimental conditions.

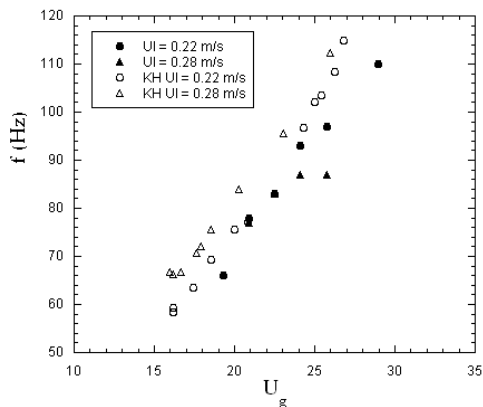


Figure 10: Frequency of the flapping instability (filled symbols) and of the Kelvin-Helmholtz instability (empty symbols) as a function of gas velocity U_g .

Though the range of gas velocity U_g is not large enough to predict a scaling of the flapping frequency with gas velocity, the experimental points are consistent with a frequency proportional to U_g . This is the scaling law experimentally measured by Lozano et al (2005)⁸ on their liquid sheet experiment (a rectangular liquid sheet atomized by two parallel gas streams). This is also the scaling found by Couderc (2007)⁹ in his numerical simulation of the same liquid sheet configuration. The analogy between their configuration and ours resides in the limit of the jet instability when the radius is decreased: for a large radius KH instability is merely a surface instability, but when R becomes of the order of magnitude of the KH instability wavelength, it can be expected that sinuous modes analogous to the flapping modes of a liquid sheet may start to overcome the axisymmetric instability in our experiment. In a flapping sheet it is known¹⁰ that the sinuous mode overcomes the varicose mode: it is relatively easier for waves on opposing sides to propagate with opposing phases (sinuous mode) than with the same phase (varicose mode).

In our configuration this has been verified by solving the inviscid stability analysis in axisymmetric geometry for helical modes of the form $e^{i(kx-\omega t+n\theta)}$ with $n \neq 0$. We solve the resulting dispersion relation for spatial modes, i.e. complex wavenumber and real frequency. We find that modes for $n=1$ are unstable. Modes for $n>1$ are all stable. The focus of this paper being on the experimental study, we just present on figure 10 the comparison of the resulting growth rate for the axisymmetric mode ($n=0$) and the helical mode ($n=1$): it can be seen that when the radius of the jet is decreased (in figure 11, R is nondimensionalized by the vorticity thickness δ), the growthrate of the helical mode overcomes that of the varicose mode. In our experimental conditions we have $R/\delta \sim 20$ (the value increases when the gas velocity is increased), which corresponds on figure 11 to the region where the helical mode is significantly more unstable than the $n=0$ mode. This predicts that the KH instability for our conditions should produce non axisymmetric surface waves.

This might be at the origin of, or at least enhance, the flapping instability: figure 12 shows a PIV visualization of the gas velocity field around the liquid jet for experimental conditions for which the flapping instability is observed farther downstream. The PIV is carried out with a laser slice of the coaxial jet, and a seeding of the gas phase with oil droplets. Figure 12 shows how the gas jet is detached from the liquid jet downstream the first KH wave, causing large gas recirculations scaling with the KH wavelength. In particular, it can be noticed how the slight dissymmetry in the KH wave (the left side of the wave is a bit ahead the right side) induces a dissymmetry in the way the gas jet impacts the liquid jet downstream the large recirculations: we suspect this is the mechanism responsible for the flapping instability. This scenario has been observed on recent 2D numerical simulations of our experimental conditions¹¹.

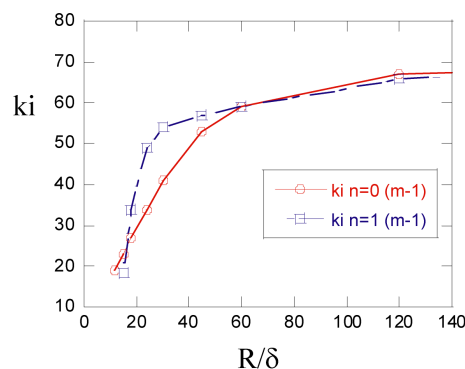


Figure 11: Result of the inviscid stability analysis in cylindrical geometry: growthrate of the unstable axisymmetric and helical modes as a function of the ratio R/δ . The helical mode has a larger growthrate.

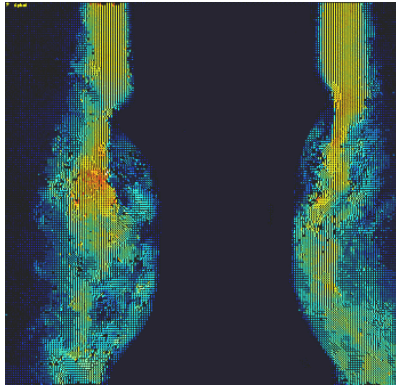


Figure 12: PIV visualization of the gas velocity field around the liquid jet: the flow is non axisymmetric. $U_G = 10$ m/s and $U_L = 0.4$ m/s.

CONCLUSION

We have studied the flapping instability of a liquid jet, an instability occurring downstream the Kelvin-Helmholtz instability when the liquid jet has not been fully atomized. We have presented measurements of the frequency of this instability, which is close to but smaller than the frequency of the KH instability. We offer a scenario for the development of the instability, based on the dissymmetry induced in the gas flow when non axisymmetric modes overcome the varicose modes. Further experiments need be carried out for different conditions (in particular different radii of the liquid jet, different gas injectors) in order to investigate more precisely this hypothesis, and to precise the scaling of the flapping frequency.

ACKNOWLEDGMENTS

We acknowledge the contribution of several undergraduate students on this experimental set-up: Angélique Sage, Antoine Delon and Aleix Poch Parera.

REFERENCES

1. Varga, Lasheras, J.C., and Hopfinger, E. J. Liquid Jet instability and atomization in a coaxial gas stream. *Annu. Rev. Fluid Mech.*, 32, 275-308, (2000).
2. Raynal, L. Instabilité et entraînement à l'interface d'une couche de mélange liquide-gaz.: PhD Thesis, UJF Grenoble France (1997).
3. Ben Rayana F., Contribution à l'étude des instabilités interfaciales liquide-gaz en atomisation assistée et tailles de gouttes, PhD Thesis, INP Grenoble France.
4. Hong, M. Atomisation et mélange dans les jets coaxiaux liquide-gaz. PhD Thesis UJF, Grenoble (2003).
5. Marmottant, P and E. Villermaux. On spray formation. *J. Fluid Mech.*, 498, (2004).
6. Hong, M., Cartellier A. & Hopfinger E.J., Atomization and mixing in coaxial injection, *Proc. 4th Int. Conf. on Launcher Technology*, Liège Belgique (2002).
7. Varga, C.M., Lasheras, J.C. and Hopfinger, E.J., Initial break-up of a small-diameter liquid jet by a high-speed gas stream, *J. Fluid Mech.*, 497, (2003).
8. Lozano, A., Barreras., F., Siegler, C. and Löw, D., The effects of sheet thickness on the oscillation of an air-blasted liquid sheet, *Experiments in Fluids*, 39, 127-139 (2005).
9. Couderc F., Développement d'un code de calcul pour la simulation d'écoulements de fluides non miscibles. Application à la désintégration assistée d'un jet liquide par un courant gazeux: PhD Thesis, ENSAE Toulouse France (2007).
10. Lin S.P., Breakup of liquid sheets and jets, Cambridge University Press, 2003.
11. Matas J.-P., Estivalezes J.-L. & Cartellier A., Atomisation gaz-liquide: lien entre l'instabilité grande-échelle d'un jet liquide et le flapping d'une nappe liquide, 2nd colloque INCA, Rouen France (2008).